chemistry

MDPI

Article

Condensed DNA Nanosphere for DNA Origami Cryptography

Rui Gao, Zhuang Cai, Jianbang Wang * and Huajie Liu *

Key Laboratory of Advanced Civil Engineering Materials of Ministry of Education, School of Chemical Science and Engineering, Shanghai Research Institute for Intelligent Autonomous Systems, Tongji University, Shanghai 200092, China

* Correspondence: wangjianbang@tongji.edu.cn (J.W.); liuhuajie@tongji.edu.cn (H.L.)

Abstract: Maintaining the confidentiality and integrity of the messages during a transmission is one of the most important aims of encrypted communication systems. Many achievements were made using biomolecules to improve the quality of the messages in communication. At the same time, it is still a challenge to construct cooperative communications based on the interactions between biomolecules to achieve the confidentiality and integrity of the transmitted messages. DNA-based encrypted communications have been developed, and in particular, DNA-origami-based message encryption can combine steganography and pattern encryption and exhibits extremely high confidentiality. Nevertheless, limited by biological characteristics, encrypted messages based on DNA require a strict storage environment in the process of transmission. The integrity of the message encoded in the DNA may be damaged when the DNA is in an unfriendly and hard environment. Therefore, it is particularly significant to improve the stability of DNA when it is exposed to a harsh environment during transmission. Here, we encoded the information into the DNA strands that were condensed for encryption to form a nanosphere covered with a shell of SiO_2, which brings high-density messages and exhibits higher stability than separated DNA. The solid shell of SiO_2 could prevent DNA from contacting the harsh environment, thereby protecting the DNA structure and maintaining the integrity of the information. At the same time, DNA nanospheres can achieve high throughput input and higher storage density per unit volume, which contribute to confusing the message strand (M-strand) with the interference strand in the stored information. Condensing DNA into the nanosphere that is used for DNA origami cryptography has the potential to be used in harsh conditions with higher confidentiality and integrity for the transmitted messages.

Keywords: encrypted communication; higher density; stability; SiO_2 shell

Citation: Gao, R.; Cai, Z.; Wang, J.; Liu, H. Condensed DNA Nanosphere for DNA Origami Cryptography. *Chemistry* **2023**, *5*, 2406–2417. https://doi.org/10.3390/chemistry5040159

Academic Editor: Di Li

Received: 15 September 2023
Revised: 4 November 2023
Accepted: 6 November 2023
Published: 8 November 2023

1. Introduction

As time passes, the issue of message security has gained significant prominence; ensuring the confidentiality and integrity of messages is an urgent issue that needs to be solved [1]. To address this issue, complex cryptographic methods that rely on challenging computational problems have been devised to facilitate secure communication [2–4]. However, the development of computer technology and the progress of hardware have made it possible to crack cryptographic protocols by brute force attacks in a short time [5]. Biomolecular cryptography utilizes highly specific thermodynamic control of biomolecular interactions to implement encryption schemes. Based on the existing technology, this type of encryption is difficult to brute-force crack in a short period. DNA, serving as a crucial repository of human genetic data, possesses inherent characteristics of exceptional precision and high information density, making it an ideal medium for message storage [6–8]. The designability of the DNA sequences provides a convenient condition for encrypting messages into the DNA and reading messages from the DNA. Clelland et al. [9,10] used this property to develop a DNA-based steganography scheme to hide secret messages, and Wong et al. [11] reported on the data storing in DNA in prokaryotic organisms. DNA data storage is a biological device that has received widespread attention for a long time [12,13].

Based on this characteristic, our research group developed the DNA origami cryptography (DOC) technology [14]. We encrypted messages into the sequential point patterns that were implemented physically through a combination of scaffold strands. By combining DOC with a steganography algorithm and pattern encryption, the confidentiality of DOC was further enhanced. Through the application of DOC technology, we've successfully achieved encrypted transmission for various types of data, including text, patterns, and musical notes.

The implementation of DOC relies on the precise identification of DNA molecules. It utilizes over 200 staple strands with 20–60 bases to precisely fold a scaffold strand consisting of more than 7000 bases into nanostructures with specific patterns, thereby revealing concealed encrypted messages [15]. The reading of the hidden message is dependent on the correct folding of the DNA nanostructures, making it particularly essential to safeguard the integrity of the nucleic acid strands during the message transmission process. However, DNA is highly sensitive to physical, chemical, and biological detrimental conditions, such as ultraviolet radiation [16], high temperature [17], strong acids and bases, as well as various nucleases that induce DNA hydrolysis, oxidation, alkylation [18], pyrimidine dimerization [19], and so on. Encasing DNA within a polymer shell coated with inorganic minerals has been demonstrated to enhance the stability of DNA in hard external conditions [20]. Especially when packaging the DNA with silica, the resistance effect is particularly obvious in the harsh environment [21–24]. According to research, DNA is the ligand for various metal ions, including Zn^{2+}, Mg^{2+}, Mn^{2+}, Ca^{2+}, Cu^{2+}, and so on [25]. Fe^{2+} ions can self-assemble to form nanoparticles driven by coordination with DNA oligonucleotides [26–28]. In addition, other metal ions [29–31] can also coordinate with DNA oligonucleotides to form nanoparticles that were used as nano-enzymes [32] with excellent catalytic activities and used as drug carriers [33–35] in vivo.

In this study, we chose to hide the encrypted message in the DNA strands and encapsulate them within the SiO_2 shell to ensure the confidentiality and integrity of the transmitted message. Differently from the reported techniques, such as DNA mineralization, we pre-compressed the DNA strands into nanospheres encoded with the message in advance, greatly improving its loading efficiency. This process could greatly increase the density of stored information. At the same time, the release density of the message strands after removing the silicon shell was increased to achieve high-throughput writing and high-throughput reading of information. Consequently, our method achieved high-throughput writing and reading of the messages. For the reading process, we used the DOC technology to decode the transmitted message, which was built to transform the encrypted message into a visual message. The DOC method not only omitted the complicated sequencing process but also introduced our encryption mechanism to form a DNA strand sequence carrying the message through the encryption of the message text. Then, the message was double encrypted by the distribution of the message strands on the DNA scaffold and the spatial folding of the scaffold strands. Once the appropriate key was acquired and the message strands were correctly positioned in space, streptavidin was used as the message display agent to carry out visual reading under Atomic Force Microscopy (AFM). This encryption method of message combined the advantages of cryptography and steganography, which not only ensured the long-term integrity of the encrypted message but also offered a high level of concealment and security during the process of message transmission.

2. Materials and Instruments

2.1. Materials and Reagents

Zinc acetate dihydrate ($C_4H_6O_4Zn{\cdot}2H_2O$), Magnesium chloride hexahydrate ($MgCl_2{\cdot}6H_2O$), Calcium chloride anhydrous ($CaCl_2$), Manganese (II) acetate tetrahydrate ($C_4H_6O_4Mn{\cdot}4H_2O$), Cobalt (II) chloride hexahydrate ($CoCl_2{\cdot}6H_2O$), Copper (II) chloride dihydrate ($CuCl_2{\cdot}6H_2O$), Iron (III) chloride hexahydrate ($FeCl_3{\cdot}6H_2O$), Iron (II) chloride ($FeCl_2$), Nickel (II) chloride hexahydrate ($NiCl_2{\cdot}6H_2O$), tetramethylammonium polysilicate (TMAPS), and tetraethoxysilane (TEOS), were purchased from Sinopharm Chemical

Reagent Co., Ltd. (Shanghai, China). Ammonium Hydrogen Fluoride ($(NH_4)HF_2$) and Ammonium Fluoride (NH_4F) were purchased from Titan Scientific Co., Ltd. (Shanghai, China). M13mp18 single-stranded DNA was purchased from Takara Bio Inc (Beijing, China). All of the synthetic oligonucleotide sequences, streptavidin, and SYBR Green I used in this study were synthesized by Sangon Biotechnology Co., Ltd. (Shanghai, China). which were purified by PAGE. All experimental water was purified by the Millipore Milli-Q integrated water purification system (Burlington, MA, USA).

The rectangular DNA origami sequence is designed from reference [36]. Detailed information on the DNA origami (Figures S1–S3) and sequence is available (Table S1). Other single-stranded DNA sequences are as follows:

Message strands (M-strands):

M_1	AGTGTACTTGAAAGTATTAAGAGGCCGCCACCTTT-bio
M_2	CCGCCAGCCATTGCAACAGGAAAAATATTTTTTTT-bio
M_3	TTTTTATAAGTATAGCCCGGCCGTCGAGTTT-bio
M_4	GCGCATTATTTTGCTTATCCGGTATTCTAAATCAGATTT-bio
M_5	CCCCGATTTAGAGCTTGACGGGGAAATCAAAATTT-bio
M_6	CAATGACACTCCAAAAGGAGCCTTACAACGCCTTT-bio
M_7	GCTAAATCTTTTCTGTAGCTCAACATGTATTGCTGATTT-bio
M_8	CAGCGAAAATTTTACTTTCAACAGTTTCTGGGATTTTTT-bio

(M_1, M_2, M_3, M_4, M_5, M_6, M_7, and M_8 was used to decode "D" characters; M_1, M_2, M_4, M_5, M_6, and M_7 was used to decode "O" characters; M_2, M_3, M_4, M_5, M_7, and M_8 was used to decode "C" characters)

Interfering strands:

I_1	GACCTGACGACATAGACTTGAGAGAGCGACTTT-bio
I_2	ACTTGAGAGAGCGACTCGACGACTACTGACTTT-bio
I_3	GCGGACATTCGCTGACCTCTCACCCACCATTTT-bio

2.2. Experimental Instruments

The samples for SEM analysis were prepared by dispersing the nanospheres in Milli-Q water and then dropping them onto a silicon substrate using Hitachi S4800 Cold field emission scanning electron microscopy (Tokyo, Japan). Dynamic light scattering (DLS) analysis was performed by a Litesizer 500 instrument (Anton Paar GmbH, Graz, Austria). X-ray photoelectron spectroscopy (XPS) measurement was performed with AXIS Ultra DLD instrument (The Shimadzu Kratos Company, Hadano, Japan). Fluorescence spectra of the samples were measured by the Hitachi F-2710 fluorescence spectrophotometer (Tokyo, Japan). UV-Vis absorption spectra of the samples were measured by the Hitachi U-2910 ultraviolet spectrophotometer (Tokyo, Japan). DNA concentration was quantified by NanoDrop One produced by Thermo Fisher Scientific (Kandel, Germany). DNA origami was characterized by atomic force scanning probe microscope (Bruker Nano Inc, Billerica, MA, USA). All samples were centrifuged by Hitachi centrifuge (Tokyo, Japan).

3. Methods

3.1. Preparation of DNA Nanospheres

A 4 mM Zn^{2+} aqueous solution and 20 μM DNA aqueous solution containing target message and interferential message were mixed and heated at 95 °C for 15 min. The sample was centrifuged at 10,000 rpm and washed three times. The supernatant was taken to determine the loading efficiency of DNA, and the precipitate was the nanosphere with the message.

3.2. Compression Ratio and Release Rate of the DNA Nanospheres

The as-formed suspension through metal ions reacted with DNA was centrifuged at 10,000 rpm for 10 min. Then, the supernatant was recorded by UV absorption at 260 nm to quantify the noncompressed DNA. Finally, the DNA compression ratio could be obtained by the following formula: DNA compression ratio = $n_{(\text{compressed DNA})}/n_{(\text{total DNA})} \times 100\%$.

DNA release ratio was measured by deconstructing the precipitate. In detail, 200 μL EDTA (100 mM) was mixed with precipitate and reacted at 25 °C for 15 min. Then, the precipitate would be dissolved, and the as-compressed DNA would be released. The released DNA was also quantified by UV-Vis. the DNA release ratio could be obtained by $n_{(\text{released DNA})}/n_{(\text{compressed DNA})} \times 100\%$.

3.3. Synthesis of Protected DNA Nanosphere

The precipitates of DNA nanospheres with the message compressed in the previous step were suspended in 500 μL water, and tetramethylammonium polysilicate (TMAPS, 50% in MeOH, 0.6 μL) as cationic co-structure directing agent was added and stirred at a room temperature. Then, tetraethoxysilane (TEOS, 99.0%, 0.6 μL) was added and reacted at room temperature for 4 h under the condition of intense agitation to co-condensation. Then, 4 μL TEOS was added and stirred at 900 rpm for 4 days to synthesize and encapsulate the silica.

3.4. DNA Release

A mixed aqueous solution (pH = 4) of 0.8 M $(NH_4)HF_2$ solution and 1 M NH_4F solution was used as the etching solution for silicon dioxide, and 100 mM EDTA solution was used to release message strands. A 20 μL etching solution was added to 5 μL Si-DNA nanosphere and reacted for 20 min, and then 15 μL EDTA solution was added for 15 min. The released DNA would be used for subsequent message reading.

3.5. Denaturing Polyacrylamide Gel Electrophoresis (dPAGE)

The nanospheres with the message were digested by Exonuclease I at 37 °C for 30 min and heated at 80 °C for 15 min (to inactivate Exonuclease I). Then, the message strands contained within nanospheres were released to assess structural integrity. The nanospheres without silica coating were directly reacted with 100 mM EDTA. The nanospheres with silica coating were first treated with the prepared etching solution. After etching, a complexation reaction was performed to release the DNA. This obtained DNA was diluted to appropriate concentration and analyzed using 15% denaturing polyacrylamide gel electrophoresis (dPAGE) with EDTA (7 M). All the electrophoresis was run under a voltage of 90 V for 1 h in 1 × MOPS buffer. After staining with SYBR Gold, the imaging was performed with the GenoSens 1800 Series gel imaging analysis system.

3.6. Reading of DNA Information

The geometry of the dot pattern covering the message was defined beforehand. We chose M13mp18 as the scaffold, and Alice's scaffold strand could be collected in the tube and delivered directly to Bob. The 200 nM M-strands and 20 nM scaffold strands were mixed in 1 × TAE buffer (40 mM Tris, 20 mM acetic acid, and 2 mM EDTA, pH 8.0) with 12.5 mM Mg^{2+}. The excess M-strands promoted complete hybridization with the scaffold. Rapid annealing of 85 °C to 4 °C was performed in the PCR procedure. The unbound M-strands were removed by an ultrafiltration centrifugal tube (Amicon, Darmstadt, Germany) with 100 kDa (Molecular Weight Cutoff–MWCO).

In the process of DNA origami, the staple was mixed with the scaffold carrying M-strands at a ten-fold overdose ratio in 1 × TAE buffer with 12.5 mM Mg^{2+}, and the final concentration of the scaffold strand was 2 nM. Subsequently, the mixture was heated at 57 °C for 3 min and then annealed by a step at a rate of −5 °C per minute until it reached 27 °C. Afterward, the folded DNA origami was subjected to three rounds of purification by centrifuge filters with 100 kDa (MWCO) to eliminate any excess strands. A ten-fold

excess of streptavidin was added to identify biotin with the single strand on DNA origami. After incubating at room temperature for 2 h, the resulting patterns were characterized under AFM.

3.7. Characterization of Patterns Using AFM

A droplet of sample (5 µL) with patterned DNA origami (2 nM) was deposited on freshly cleaved mica surface and left to absorb for 5 min. Then, 40 µL 1 × TAE buffer with 12.5 mM Mg^{2+} was added to the liquid cell, and a fluid^{+} (Bruker, Inc.) tip was used to image the sample in ScanAsyst in fluid mode on a Multimode VIII AFM (Bruker Nano Inc.).

4. Result and Discussion

4.1. The Principles of Encrypted Communication

The schematic diagram of condensed DNA encrypted information transmission is shown in Figure 1. We assumed that two virtual characters, Alice and Bob, were conducting encrypted communication. Alice first encoded the transmitted plaintext information into a nucleic acid base sequence to obtain a message strand and modified biotin at one end of the message strand to facilitate the reading of the subsequent message. Then, the message strands were mixed with the interfering message strands, and Zn^{2+} ions were used to compress the mixed DNA strands into the message nanosphere. Compared with previous studies, the loading efficiency of DNA was improved, and high-throughput input of conveying information and interference information can be achieved with a lower concentration of message nanospheres. Subsequently, the DNA nanospheres were wrapped in a silicon shell to withstand the harsh environment during encrypted transmission and improve the stability of the information. After receiving the message nanospheres, Bob released all the correct messages and incorrect messages from the nanosphere coated with a SiO_2 shell. Then, a pre-agreed upon scaffold strand was utilized to screen and identify the accurate M-strands, and the correct staple strands were introduced to guide the scaffold strand folding, ensuring the M-strands were positioned correctly in space. Finally, streptavidin was used to combine with biotin on the M-strands to generate a prefabricated pattern on the DNA origami to achieve a visual reading of the hidden message.

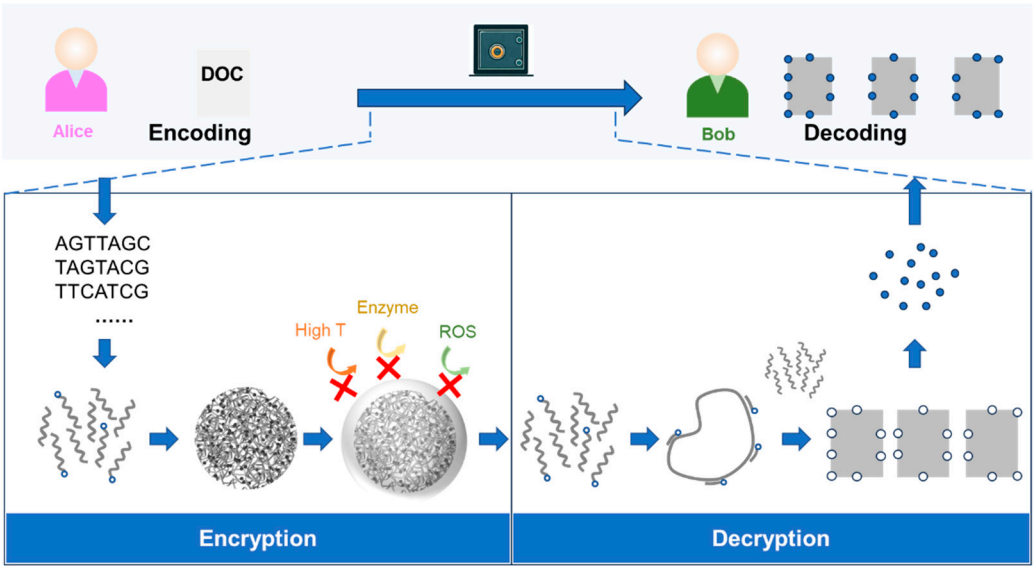

Figure 1. Schematic diagram of the encrypted communication between Alice and Bob.

4.2. Preparation of DNA Nanospheres

Enriching dispersed DNA has been proven to be an effective means to achieve information storage. The methods based on adsorbing DNA onto nanoparticles for information storage have been established in recent years. However, these methods still face the problem

of low DNA loading rate [22,37,38]. In order to achieve high-throughput input of messages, we proposed the use of nanospheres composed of DNA for message transmission. First, message nanospheres with higher DNA density were prepared to greatly improve weight loading (weight of DNA as a percentage of total weight) in terms of data density. The abundant coordination sites on the DNA bases facilitated the bounding of the metal ions to the negatively charged phosphate scaffold. Coordination-driven self-assembly occurred in thermal environments and compressed the soft DNA strands to form the DNA nanosphere (as shown in Figure 2a). These nanospheres could be easily separated from the liquid phase by centrifugation. Based on this standard, we tried nine metal ions that could coordinate with DNA to select the best metal ions for DNA nanosphere preparation.

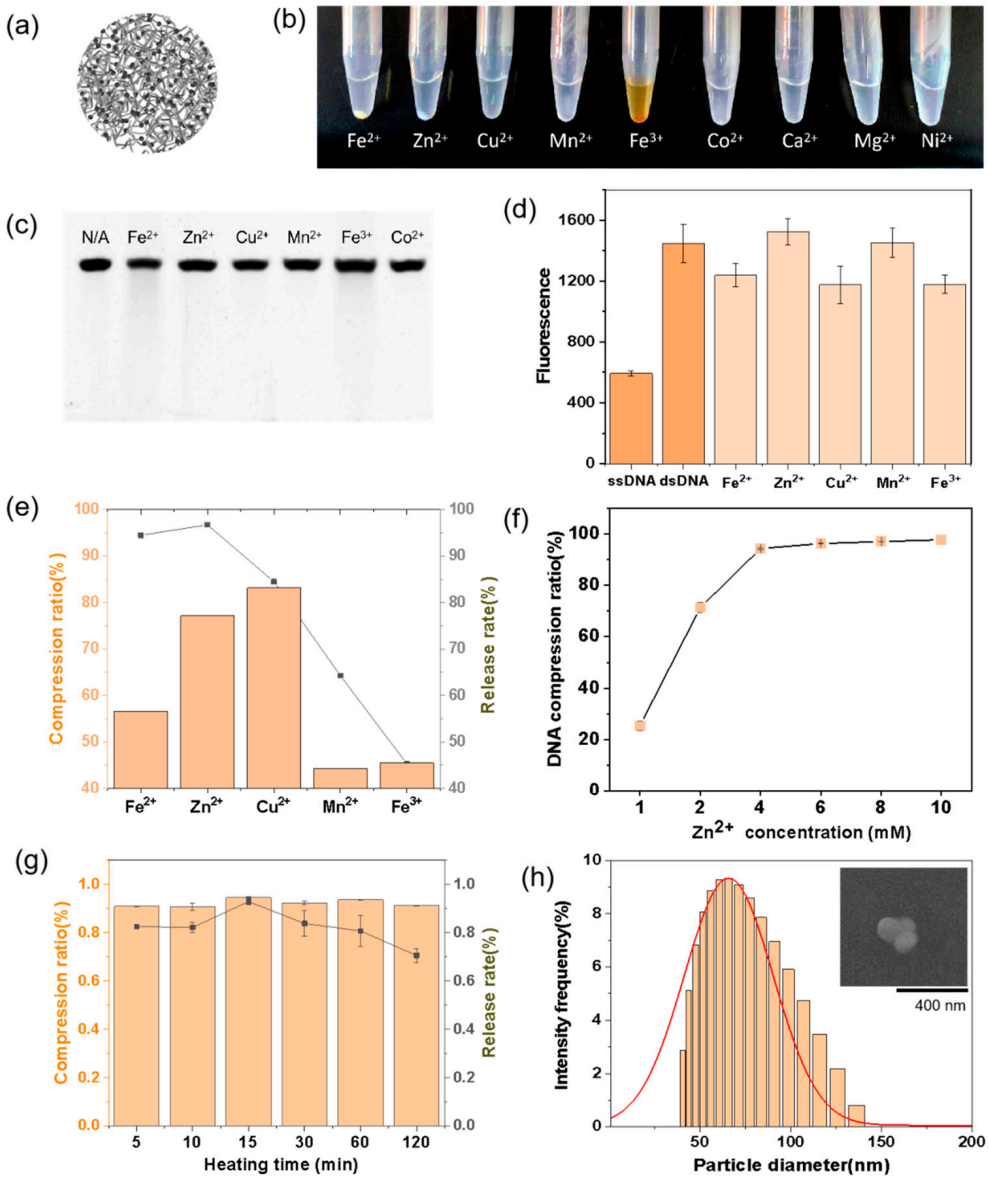

Figure 2. (**a**) Schematic diagram of DNA nanosphere; (**b**) optical image of nanosphere precipitation formed by different metal ions with DNA; (**c**) dPAGE diagram of DNA strands released by DNA nanosphere prepared by different metals; (**d**) fluorescence intensity diagram of DNA released by DNA nanosphere prepared by different metals after hybridization to form double strand stained by SGI; (**e**) diagram of DNA compression and release rate of different metal ions; (**f**) trend diagram of DNA compressibility of Zn^{2+} at different concentrations; (**g**) compressibility and corresponding release rate of 4 mM Zn^{2+} compressed DNA at different times; and (**h**) particle size distribution of DNA nanosphere. The inserted image was the SEM image of the corresponding DNA nanosphere.

As shown in Figure 2b, different types of metal ions at the same concentration were mixed with DNA, and the solutions were heated at 95 °C for 15 min and then centrifuged 1at 10,000 rpm for 10 min. Fe^{2+}, Zn^{2+}, Cu^{2+}, Mn^{2+}, and Fe^{3+} all formed visible precipitates with DNA, demonstrating the successful formation of the DNA nanosphere.

Next, we explored whether these metal ions affect the structural integrity of DNA. It had been reported that metal ions had the potential to cleave DNA [39], so we used EDTA to decompress DNA nanospheres formed by different metal ions and release the DNA strands for gel electrophoresis experiments. As shown in Figure 2c, DNA nanospheres were placed in an aqueous solution for 3 days, and the released DNA strands still maintained their structural integrity.

To further rule out the possibility of base damage, hybridization experiments were used for evaluation. SYBR Green I(SGI) dyes could specifically stain DNA double strands. If the integrity of the bases is damaged, a complete base pair cannot be formed, and the corresponding fluorescence intensity will also decrease. We explored the sensitivity of the SGI to DNA base mismatches. As shown in Figure S4, when there was a base mismatch, there would be a corresponding fluorescence intensity decrease. The more mismatched bases there were, the more the fluorescence intensity decreased, and there was a nonlinear downward trend.

As shown in Figure 2d, the samples corresponding to Zn^{2+} and Mn^{2+} exhibited fluorescence intensities similar to double-stranded DNA (dsDNA), indicating that the integrity of the DNA bases was maintained. Next, the efficiency of DNA compression and release was investigated. The amount of DNA variation in the precipitated supernatant was quantified to explore the efficiency of compression. Cu^{2+} and Zn^{2+} showed high compression efficiency. DNA in the nanospheres was released to measure the DNA content of the supernatant; Fe^{2+} and Zn^{2+} showed better release efficiency, as shown in Figure 2e. In conclusion, Zn^{2+} was a good choice for the preparation of the DNA nanosphere compression. Therefore, we explored the optimal conditions for the preparation of DNA nanosphere by Zn^{2+}. As shown in Figure 2f, the yield of the DNA nanosphere increased with the concentration of Zn^{2+}, reaching an optimal concentration of 4 mM. The compression of DNA nanospheres showed fast dynamics, and the compression of DNA nanosphere was completed in 5 min. The structural stability was maintained over a long period of time (Figure 2g). The release rate of DNA had the best performance at 15 min, so the best condition for preparing DNA nanospheres was determined, which was 4 mM of reaction concentration and 15 min of the reaction time. Additionally, DLS results indicated that the size of the DNA nanospheres was approximately 72 nm, which aligned with SEM results (Figure 2h).

4.3. Preparation of Si-DNA Nanospheres

The DNA nanosphere with negative charge was combined with TMAPS through charge interaction. A small amount of TEOS was first added for pre-nucleation, and then more TEOS was added subsequently to further guide the growth of the SiO_2 shell during vibration (Figure 3a). The size of Si-DNA nanospheres coated with SiO_2 became larger. DLS data showed that the size of Si-DNA nanospheres was about 80 nm. SEM image further validated this size characteristic, as shown in Figure 3b. The successful growth of SiO_2 on the DNA nanosphere surface could also be demonstrated by XPS data. As shown in Figure 3c, the DNA nanospheres showed the characteristic peak of DNA at 168.9 eV for P 2p and 192.9 eV for P 2s, while a strong characteristic peak of Zn^{2+} was observed at 1022.9 eV for Zn $2P_{3/2}$, 1044.9 eV for Zn $2P_{1/2}$, and 1230.9 eV for Zn 2S. However, the Si-DNA nanospheres could only observe the characteristic peaks of SiO_2, corresponding to Si $2P_{1/2}$ at 103.6 eV and Si 2S at 154.6 eV, respectively; the characteristic peaks of Zn could not be observed. It indicated that SiO_2 successfully formed a shell on the surface of the DNA nanosphere, and the DNA was protected inside.

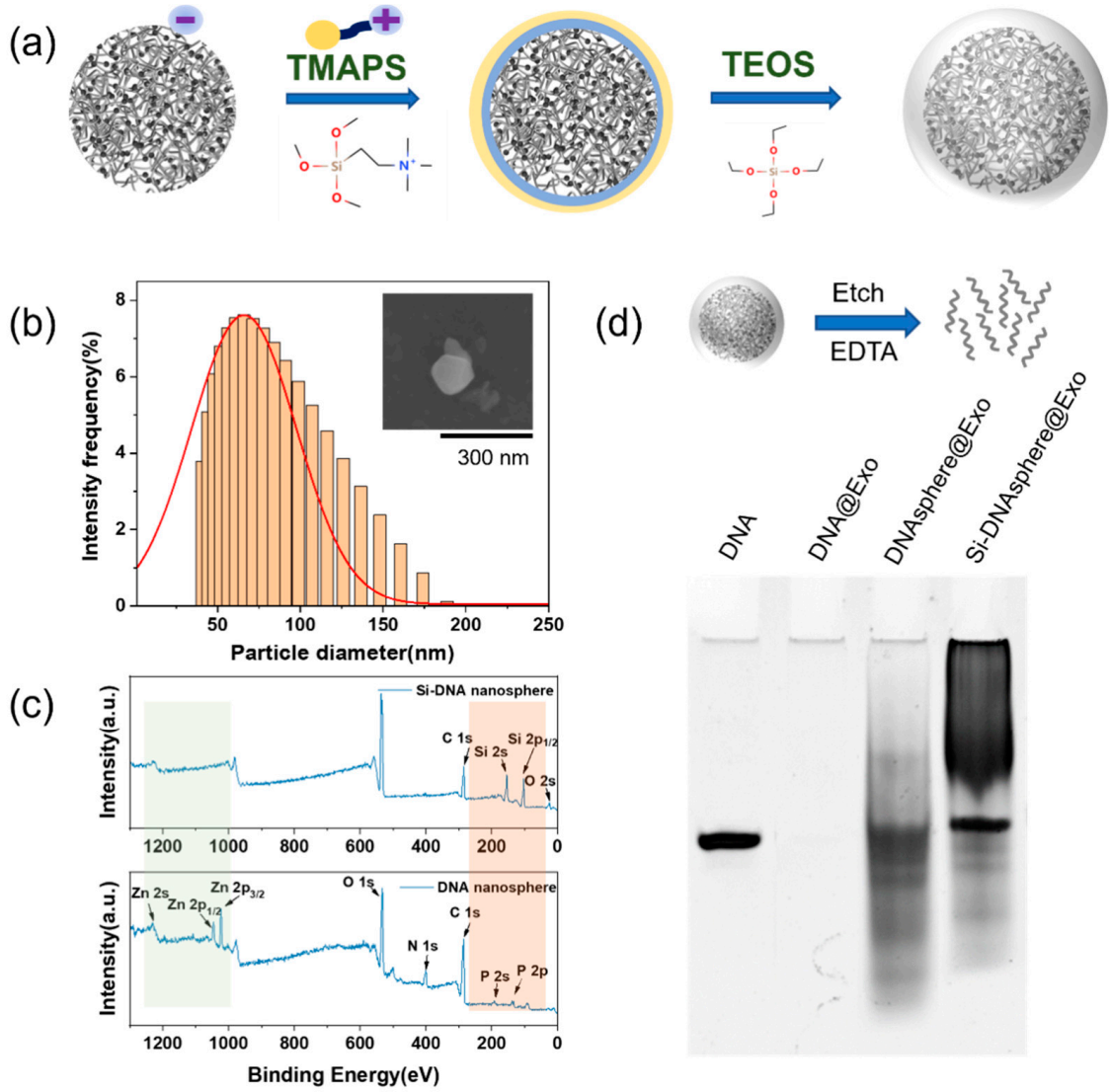

Figure 3. (**a**) Schematic diagram of SiO_2 shell growth of DNA nanosphere; (**b**) Particle size distribution of Si-DNA nanosphere. The inserted picture was the SEM image of the corresponding Si-DNA nanosphere. (**c**) XPS map of DNA nanosphere and Si-DNA nanosphere; (**d**) dPAGE diagram of DNA strand after Exonuclease I treatment.

We further verified the ability of the Si-DNA nanosphere to protect internal DNA. High temperature, ROS, and enzymes are all important factors affecting DNA integrity. Studies have shown that nanospheres formed by metal ions coordinated with DNA could withstand long-term heat treatment [30]. Grass et al. also confirmed that silica can resist high temperature and ROS damage to DNA by qPCR analysis [22]. Compared with lots of harsh environments, enzyme cutting had the worst structural damage to DNA, so Exonuclease I was selected as the destroyer to damage DNA. Exonuclease I was applied to untreated ssDNA, DNA nanospheres, and Si-DNA nanospheres for a 30 min pretreatment, respectively, and then the integrity of DNA in the DNA nanosphere and Si-DNA nanosphere was released for evaluation via gel electrophoresis. As shown in Figure 3d, the DNA was completely destroyed after being treated by Exonuclease I, while part of the DNA in the DNA nanosphere was preserved, and the DNA in the Si-DNA nanosphere was mostly preserved. It proved that Si-DNA nanospheres could effectively protect the M-strand wrapped in it. The band tailing of Si-DNA nanosphere@ Exo might be due to the silicates and fluoride ions produced by etching away the silicon dioxide in the released DNA solution, which

would form larger complexes with the substances in the gel. However, it does not affect the hybridization ability of the M-strand.

4.4. Reading of Encrypted Information in the Si-DNA Nanosphere

The silicon shell on the surface of the DNA nanospheres could be successfully etched by a mixture of $(NH_4)HF_2$ and NH_4F. As shown in Figure 4a, DNA inside the DNA nanosphere was released by EDTA after etching. The scaffold strand recognized the correct message strand and pre-hybridized with it, placing the message strands at the correct position of the scaffold strand.

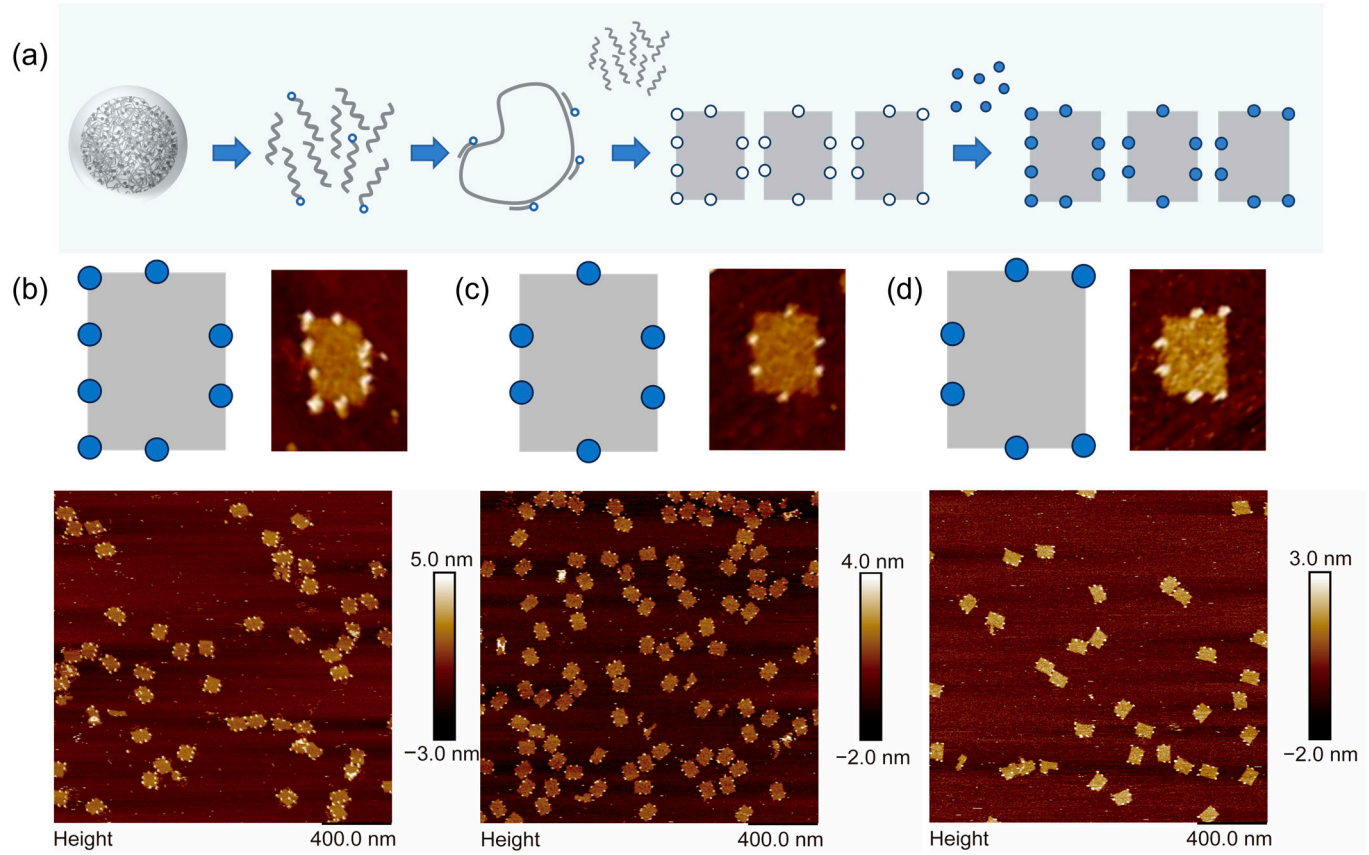

Figure 4. (**a**) Schematic diagram of the process of obtaining plaintext patterns by decrypting DNA nanospheres; (**b**) decrypted AFM images corresponding to D characters; (**c**) decrypted AFM images corresponding to O characters; and (**d**) decrypted AFM images corresponding to C characters.

The scaffold strand carrying the M-strands was then annealed with a set of universal staple strands to form an origami structure. Biotin molecules were strategically placed at predetermined locations on the surface of the DNA origami. Then, streptavidin was added to hybridize with biotin. Streptavidin could display these biotin sites with messages under AFM imaging, thereby obtaining the information of the encrypted strands, that is, the pattern information to be transmitted. We encrypted the text of D, O, and C, respectively, hid their corresponding point message in the DNA nanospheres, and decoded the encrypted message by the above method. As shown in Figure 4b–d, DNA origami showed distinct lattice patterns under AFM imaging, which composed the text words of D (Figure 4b), O (Figure 4c), and C (Figure 4d), respectively. The information contained within the silicon shell package is largely preserved (Figures S5–S10).

5. Conclusions

This work improved the loading efficiency of DNA by DNA nanospheres, thereby increasing the data density and realizing high-throughput storage of information. The

mixture of M-strands and interference strands successfully achieved the first level of encryption information hiding. After forming the nanosphere, the DNA was successfully wrapped in a silicon shell to resist the adverse external environment, greatly reducing the possibility of DNA damage during information transmission and ensuring the integrity of information storage. At the same time, the DOC system we developed previously was employed for decoding the information, completing the second layer of encryption. Successful integration of the sequence encryption and steganography achieved a multi-level encryption. The feasibility of this method was demonstrated using a "DOC" text message as an example. Furthermore, the application potential of DNA origami shape design and surface addressability provides many possibilities for this method of information encryption. This method of information storage can be preserved for a long time and is conducive to transmission. In the future, it may be used as an effective alternative to the information transmission and storage methods that are currently under serious threat.

Supplementary Materials: The following supporting information can be downloaded at https://www.mdpi.com/article/10.3390/chemistry5040159/s1. Figure S1: Schematic diagram of the formation of pattern D on DNA origami; Figure S2: Schematic diagram of the formation of pattern O on DNA origami; Figure S3: Schematic diagram of the formation of pattern C on DNA origami; Figure S4: Test the sensitivity of SYBR Green I dye to single-stranded DNA base damage. There was a significant decrease in fluorescence intensity for mismatches of 1, 3, 5, 7, and 9 bases; Figure S5: Pattern D revealed by DNA origami after release from the DNA nanospheres without silica coating, and its yield; Figure S6: Pattern D revealed by DNA origami after release from the DNA nanospheres with silica coating, and its yield; Figure S7: Pattern O revealed by DNA origami after release from the DNA nanospheres without silica coating, and its yield; Figure S8: Pattern O revealed by DNA origami after release from the DNA nanospheres with silica coating, and its yield; Figure S9: Pattern C revealed by DNA origami after release from the DNA nanospheres without silica coating, and its yield; Figure S10: Pattern C revealed by DNA origami after release from the DNA nanospheres with silica coating, and its yield; Table S1: DNA origami sequence; Table S2: Mismatched bases sequence used to test SGI dyes.

Author Contributions: Conceptualization, R.G.; Methodology, R.G., Z.C. and H.L.; Formal analysis, R.G.; Investigation, R.G. and Z.C.; Data curation, R.G.; Writing—original draft, R.G. and Z.C.; Writing—review and editing, R.G., Z.C., J.W. and H.L.; Visualization, R.G., Z.C., J.W. and H.L.; Supervision, R.G., J.W. and H.L.; Project administration, R.G. and H.L.; Funding acquisition, H.L. All authors have read and agreed to the published version of the manuscript.

Funding: This work was financially supported by the National Natural Science Foundation of China (21873071, 22272119), the Science and Technology Committee of Shanghai Municipality (2022-4-ZD-03), the Shanghai Pilot Program for Basic Research, and the Fundamental Research Funds for the Central Universities.

Data Availability Statement: Data are contained within the article and Supplementary Materials.

Conflicts of Interest: The authors declare no conflict of interest.

References

1. Wu, X.; Du, Y.; Fan, T.; Guo, J.; Ren, J.; Wu, R.; Zheng, T. Threat analysis for space information network based on network security attributes: A review. *Complex Intell. Syst.* **2023**, *9*, 3429–3468. [CrossRef]
2. Sarkar, T.; Selvakumar, K.; Motiei, L.; Margulies, D. Message in a molecule. *Nat. Commun.* **2016**, *7*, 11374. [CrossRef] [PubMed]
3. Han, S.; Bae, H.J.; Kim, J.; Shin, S.; Choi, S.-E.; Lee, S.H.; Kwon, S.; Park, W. Lithographically Encoded Polymer Microtaggant Using High-Capacity and Error-Correctable QR Code for Anti-Counterfeiting of Drugs. *Adv. Mater.* **2012**, *24*, 5924–5929. [CrossRef] [PubMed]
4. Li, Y.; Zhou, X.; Yang, Q.; Li, Y.; Li, W.; Li, H.; Chen, S.; Li, M.; Song, Y. Patterned photonic crystals for hiding information. *J. Mater. Chem. C.* **2017**, *5*, 4621–4628. [CrossRef]
5. Diffie, W.; Hellman, M.E. Exhaustive Crypt-Analysis of Nbs Data Encryption Standard. *Computer* **1977**, *10*, 74–84. [CrossRef]
6. Nguyen, H.H.; Park, J.; Park, S.J.; Lee, C.S.; Hwang, S.; Shin, Y.B.; Ha, T.H.; Kim, M. Long-Term Stability and Integrity of Plasmid-Based DNA Data Storage. *Polymers* **2018**, *10*, 28. [CrossRef]

7. Church, G.M.; Gao, Y.; Kosuri, S. Next-Generation Digital Information Storage in DNA. *Science* **2012**, *337*, 1628. [CrossRef] [PubMed]
8. Goldman, N.; Bertone, P.; Chen, S.; Dessimoz, C.; LeProust, E.M.; Sipos, B.; Birney, E. Towards practical, high-capacity, low-maintenance information storage in synthesized DNA. *Nature* **2013**, *494*, 77–80. [CrossRef]
9. Clelland, C.T.; Risca, V.; Bancroft, C. Hiding messages in DNA microdots. *Nature* **1999**, *399*, 533–534. [CrossRef]
10. Bancroft, C.; Bowler, T.; Bloom, B.; Clelland, C.T. Long-Term Storage of Information in DNA. *Science* **2001**, *293*, 1763–1765. [CrossRef]
11. Wong, P.C.; Wong, K.K.; Foote, H. Organic data memory using the DNA approach. *Commun. ACM* **2003**, *46*, 95–98. [CrossRef]
12. Ailenberg, M.; Rotstein, O. An improved Huffman coding method for archiving text, images, and music characters in DNA. *Biotechniques* **2009**, *47*, 747–754. [CrossRef] [PubMed]
13. Cox, J.P. Long-term data storage in DNA. *Trends Biotechnol.* **2001**, *19*, 247–250. [CrossRef]
14. Zhang, Y.; Wang, F.; Chao, J.; Xie, M.; Liu, H.; Pan, M.; Kopperger, E.; Liu, X.; Li, Q.; Shi, J.; et al. DNA origami cryptography for secure communication. *Nat. Commun.* **2019**, *10*, 5469. [CrossRef] [PubMed]
15. Voigt, N.V.; Tørring, T.; Rotaru, A.; Jacobsen, M.F.; Ravnsbæk, J.B.; Subramani, R.; Mamdouh, W.; Kjems, J.; Mokhir, A.; Besenbacher, F.; et al. Single-molecule chemical reactions on DNA origami. *Nat. Nanotechnol.* **2010**, *5*, 200–203. [CrossRef]
16. Fang, W.; Xie, M.; Hou, X.; Liu, X.; Zuo, X.; Chao, J.; Wang, L.; Fan, C.; Liu, H.; Wang, L. DNA Origami Radiometers for Measuring Ultraviolet Exposure. *J. Am. Chem. Soc.* **2020**, *142*, 8782–8789. [CrossRef] [PubMed]
17. Lindahl, T.; Nyberg, B. Heat-induced deamination of cytosine residues in deoxyribonucleic acid. *Biochemistry* **1974**, *13*, 3405–3410. [CrossRef]
18. Koag, M.-C.; Jung, H.; Kou, Y.; Lee, S. Bypass of the Major Alkylative DNA Lesion by Human DNA Polymerase η. *Molecules* **2019**, *24*, 3928. [CrossRef] [PubMed]
19. Knips, A.; Zacharias, M. Both DNA global deformation and repair enzyme contacts mediate flipping of thymine dimer damage. *Sci. Rep.* **2017**, *7*, 41324. [CrossRef]
20. Athanasiadou, D.; Carneiro, K.M.M. DNA nanostructures as templates for biomineralization. *Nat. Rev. Chem.* **2021**, *5*, 93–108. [CrossRef]
21. Grass, R.N.; Heckel, R.; Puddu, M.; Paunescu, D.; Stark, W.J. Robust chemical preservation of digital information on DNA in silica with error-correcting codes. *Angew. Chem. Int. Ed.* **2015**, *54*, 2552–2555. [CrossRef] [PubMed]
22. Paunescu, D.; Fuhrer, R.; Grass, R.N. Protection and deprotection of DNA--high-temperature stability of nucleic acid barcodes for polymer labeling. *Angew. Chem. Int. Ed.* **2013**, *52*, 4269–4272. [CrossRef] [PubMed]
23. Chen, W.D.; Kohll, A.X.; Nguyen, B.H.; Koch, J.; Heckel, R.; Stark, W.J.; Ceze, L.; Strauss, K.; Grass, R.N. Combining Data Longevity with High Storage Capacity—Layer-by-Layer DNA Encapsulated in Magnetic Nanoparticles. *Adv. Funct. Mater.* **2019**, *29*, 1901672. [CrossRef]
24. Nguyen, M.-K.; Nguyen, V.H.; Natarajan, A.K.; Huang, Y.; Ryssy, J.; Shen, B.; Kuzyk, A. Ultrathin Silica Coating of DNA Origami Nanostructures. *Chem. Mater.* **2020**, *32*, 6657–6665. [CrossRef]
25. Sigel, R.K.; Sigel, H. A stability concept for metal ion coordination to single-stranded nucleic acids and affinities of individual sites. *Acc. Chem. Res.* **2010**, *43*, 974–984. [CrossRef] [PubMed]
26. Li, M.; Wang, C.; Di, Z.; Li, H.; Zhang, J.; Xue, W.; Zhao, M.; Zhang, K.; Zhao, Y.; Li, L. Engineering Multifunctional DNA Hybrid Nanospheres through Coordination-Driven Self-Assembly. *Angew. Chem. Int. Ed.* **2019**, *58*, 1350–1354. [CrossRef] [PubMed]
27. Yang, W.; Zhu, L.; Yang, M.; Xu, W. Synthesis of Amorphous/Crystalline Hetero-Phase Nanozymes With Peroxidase-Like Activity by Coordination-Driven Self-Assembly for Biosensors. *Small* **2023**, *19*, 2204782. [CrossRef]
28. Liu, B.; Hu, F.; Zhang, J.; Wang, C.; Li, L. A Biomimetic Coordination Nanoplatform for Controlled Encapsulation and Delivery of Drug-Gene Combinations. *Angew. Chem. Int. Ed.* **2019**, *58*, 8804–8808. [CrossRef]
29. Han, Q.; Zhang, X.; Jia, Y.; Guo, S.; Zhu, J.; Luo, S.; Na, N.; Ouyang, J. Synthesis and Characteristics of Self-Assembled Multifunctional Ln(3+) -DNA Hybrid Coordination Polymers. *Chemistry* **2022**, *28*, 202200281. [CrossRef]
30. Lu, C.; Xu, Y.; Huang, P.J.; Zandieh, M.; Wang, Y.; Zheng, J.; Liu, J. Protection of DNA by metal ions at 95 degrees C: From lower critical solution temperature (LCST) behavior to coordination-driven self-assembly. *Nanoscale* **2022**, *14*, 14613–14622. [CrossRef]
31. Lee, W.K.; Kwon, K.; Choi, Y.; Lee, J.S. Dynamic metallization of spherical DNA via conformational transition into gold nanostructures with controlled sizes and shapes. *J. Colloid Interface Sci.* **2021**, *594*, 160–172. [CrossRef]
32. Du, Z.; Zhu, L.; Wang, P.; Lan, X.; Lin, S.; Xu, W. Coordination-Driven One-Step Rapid Self-Assembly Synthesis of Dual-Functional Ag@Pt Nanozyme. *Small* **2023**, *19*, 2301048. [CrossRef] [PubMed]
33. Jia, Y.; Shen, X.; Sun, F.; Na, N.; Ouyang, J. Metal-DNA coordination based bioinspired hybrid nanospheres for in situ amplification and sensing of microRNA. *J. Mater. Chem. B* **2020**, *8*, 11074–11081. [CrossRef] [PubMed]
34. Lin, L.; Yu, J.; Lu, H.; Wei, Z.; Chao, Z.; Wang, Z.; Wu, W.; Jiang, H.; Tian, L. Mn-DNA coordination of nanoparticles for efficient chemodynamic therapy. *Chem. Commun.* **2021**, *57*, 1734–1737. [CrossRef] [PubMed]
35. Feng, X.; Liu, B.; Zhou, Z.; Li, W.; Zhao, J.; Li, L.; Zhao, Y. Engineering hierarchical metal-organic@metal-DNA heterostructures for combinational tumor treatment. *Nano Res.* **2023**. [CrossRef]
36. Fu, J.; Liu, M.; Liu, Y.; Woodbury, N.W.; Yan, H. Interenzyme substrate diffusion for an enzyme cascade organized on spatially addressable DNA nanostructures. *J. Am. Chem. Soc.* **2012**, *134*, 5516–5519. [CrossRef]

37. Antkowiak, P.L.; Koch, J.; Nguyen, B.H.; Stark, W.J.; Strauss, K.; Ceze, L.; Grass, R.N. Integrating DNA Encapsulates and Digital Microfluidics for Automated Data Storage in DNA. *Small* **2022**, *18*, 2107381. [CrossRef]
38. Ramos-Valle, A.; Marín-Caba, L.; Hevia, L.G.; Correa-Duarte, M.A.; Fanarraga, M.L. One-pot synthesis of compact DNA silica particles for gene delivery and extraordinary DNA preservation. *Mater. Today* **2023**, *18*, 100357. [CrossRef]
39. Sreedhara, A.; Cowan, J.A. Catalytic hydrolysis of DNA by metal ions and complexes. *J. Biol. Inorg. Chem.* **2001**, *6*, 337–347. [CrossRef]